

Entropy generation analysis for chemically reactive flow of Sutterby nanofluid considering radiation aspects

Waqar Azeem Khan^{a,b*}, Nazash Anjum^b, Aatef Hobiny^b and Mehboob Ali^b

^aNonlinear Analysis and Applied Mathematics (NAAM) Research Group, Department of Mathematics, Faculty of Science, King Abdulaziz University, P. O. Box 80207, Jeddah 21589, Saudi Arabia

^bDepartment of Mathematics, Mohi-ud-Din Islamic University, Nerian Sharif, Azad Jammu and Kashmir 12010, Pakistan

Abstract: Nanofluids show greater heat transfer rate and characteristics of mechanical friction diminution using nano-sized hard elements to fluid. Moreover, regarding the working of heat transfer fluid, nanofluid is widely used in areas of refrigeration, shipping, automobile, chemical industry, energy, electronics, air conditioning, computer, and many other areas to cope heat transference issues. The aforesaid utilizations motivated us to encounter entropy generation aspects for Sutterby nanofluid flow configured by permeable surface. Moreover, well-known Buongiorno's model capturing same attributes of Brownian and thermophoretic-diffusions is presented for modeling and investigation. Additionally, (MHD) as well as thermal radiation effects are the part of current work. Here, we have also considered the viscous dissipation aspects. Similarity variable are used to decrease set of nonlinear PDEs into set of ODEs then resolved numerically by using bvp4c algorithm, besides the pertinent parameters are addressed graphically. The physical aspect of fluid flow, temperature, concentration for variation of involved parameters is explained with the help of graphs.

Keywords: Sutterby nanoliquid, Entropy generation, viscous dissipation, Activation energy,

* wagarazeem@bit.edu.cn, wagar_gau85@yahoo.com

GDQM Technique.

1. Introduction

The nano fluids theory was firstly initiated by Choi [1]. In fact, nanofluids show greater heat transport and features of mechanical friction diminution via introducing nano solid particles to fluid. Nanofluid is more often used for shipping purpose, refrigeration, energy, chemical industry, electronics, air conditioning, computer, and many other regions to measure the heat transference phenomenon with lubrication requirements of great heat encumber of heat replacing structure which has simple association for economy enhancement, reduction and sustainability of heat replacing structure and has extensive applications prospects and potentially great competence economic value. By using the features of nanoparticles, Oztop and Abu Nada [2] studied convection on hot surfaces. For further expansion, Sheikholeslami *et al.* [3] conducted the same study on magnetic nanofluids. Khan *et al.* [4] deliberated the MHD flow of a Oldroyd-B nanofluid on a radially stretched convective sheet using heat generation/absorption. In recent years, the importance of nano-fluids in the field of engineering sciences is growing day by day. In present time, nano materials have inclusive range of uses in thermal phenomenon, such as crushing processes, heat exchangers, cooling engines, aerospace technology and machinery. Makinde *et al.* [5] explored the consequence of a radiative heat of variable viscous nanofluid have convective boundary conditions at the surface. Khan *et al.* [6] discussed the flow of nano-fluids through a surface of variable thickness. Adding nanoparticles to the base fluid is best for improving the efficiency of solar collectors. Mahanthesh *et al.* [7] explored the chemically reacting nanofluid flow characteristics used in colloidal analysis are taken into account using the dipole movement passing through the permeable vertical plate. Khan *et al.* [8] demonstrated effects of chemical procedures against magneto nanoparticle for the generalized Burgers fluid. Mahanthesh *et al.* [9]

discussed the different aspects of the radiator source and the radiation process as the nanofluid flows with in the turntable. Furthermore, current investigations under nanofluid dynamics contain refs. [10-31].

Efficiency of any system can be affected through the production of entropy because it reduces the outcomes of the scheme. For well presentation of system, it is essential to minimize the entropy of system. Entropy-generation is always perceived in any irreversible system whereas remains fix in any reversible system. Moreover, 2nd law of thermo-dynamics show vital role for the optimization of entropy-generation. In (1996) the basic idea about entropy-generation minimization can be functional for designing lagging /storing methods, power generation, heat exchangers and preservation methods. Majority of the entropy generation treats the convection procedures which exhibit that the entropy generation is the outcome of liquid resistance as well as heat and mass transferences phenomenon. In pure conduction methods, few papers are dealing with entropy generation. The research of Khan et al. [32-34] noticeably verified that scholars and progresses in exhibiting and simulation of entropy-generation for dissipative cross fluid by quartic autocatalysis and transportation of radiative-heat in dissipative Cross model with entropy-generation as well as activation energy. Recently, Shahzad *et al.* [35], Zhao *et al.* [36] and Qayyum *et al.* [37], Wang et al. [38] worked against entropy generation in fluid flow of viscous and non-Newtonian things focus on different geometries. The consequences are found using numerical as well as logical techniques for flow fields and show pictorially. Total entropy generation rate is achieved against stretchable Riga wall, chemical reaction and cylindrical surface. Khan *et al.* [39] reflected that heat and entropy-generation in flow featuring Robin condition. In recent times, Qayyum et al. [40], Shah et al. [41], Hussain *et al.* [42] and Waqas et al. [43] considered entropy-generation under non-linear thermal-radiation, first-order velocity slip and heat as well as mass transference in

MHD stagnation-point flow of a tangent hyperbolic nano-fluid respectively.

The objective of current study is to model the heat-mass transference aspects of magneto hydrodynamic. Sutterby nanofluid flow toward stretching sheet with simultaneous features of entropy generation and thermal radiation is under consideration. The non-linear ODEs of third-order are obtained via implementation of self-similar transformations. GDQM (Generalized differential quadrature method) technique is used to tackle the equations of the problem. The comparison tables have been computed through both schemes. Besides, the graphs are exhibited to communicate the features of non-dimensional quantities.

2. Formulation

Here, we considered the incompressible Sutterby nanofluid flow over a porous sheet along with magnetic field. Due to less magnetic Reynolds number assumption electric-field influence is overlooked. Entropy generation effect is exploited to measure the temperature features. The energy equation is based on thermophoresis, thermal radiation and Brownian movement influences.

$$\frac{\partial u}{\partial x} + \frac{\partial v}{\partial y} = 0, \quad (1)$$

$$u \frac{\partial u}{\partial x} + v \frac{\partial u}{\partial y} = \nu \left(1 - \frac{\beta^2}{6} \frac{\partial u}{\partial y} \right)^n \frac{\partial^2 u}{\partial y^2} - \left(\frac{n\nu\beta^2}{6} \right) \left(1 - \frac{\beta^2}{6} \frac{\partial u}{\partial y} \right) \frac{\partial u}{\partial y} \frac{\partial^2 u}{\partial y^2} - \frac{\sigma\beta_0^2}{\rho} u, \quad (2)$$

$$u \frac{\partial T}{\partial x} + v \frac{\partial T}{\partial y} = \frac{\nu}{c_p} \left(1 - \frac{\beta^2}{6} \frac{\partial u}{\partial y} \right)^n \left(\frac{\partial u}{\partial y} \right)^2 + \alpha \frac{\partial^2 T}{\partial y^2} + \tau \frac{D_r}{T_\infty} \left(\frac{\partial T}{\partial y} \right)^2 + \tau D_B \frac{\partial C}{\partial y} \frac{\partial T}{\partial y} - \frac{1}{(\rho c)_f} \frac{\partial q_r}{\partial y} \quad (3)$$

$$u \frac{\partial C}{\partial x} + v \frac{\partial C}{\partial y} + w \frac{\partial C}{\partial z} = \frac{D_r}{T_\infty} \frac{\partial^2 T}{\partial y^2} + D_B \frac{\partial^2 C}{\partial y^2} - k_r^2 \left(\frac{T}{T_\infty} \right)^m (C - C_\infty) \exp\left(-\frac{E_a}{KT}\right), \quad (4)$$

with

$$u = U_w = cx, \quad v = 0, T = T_w, \quad C = C_w \quad \text{at } y = 0, \quad (5)$$

$$u = U_e = cx, \quad T \rightarrow T_\infty, \quad C \rightarrow C_\infty \quad \text{as } y \rightarrow \infty. \quad (6)$$

Transformations:

$$\begin{aligned} \eta &= y \sqrt{\frac{c}{\nu}}, \quad u = cx f'(\eta), \quad v = -\sqrt{c\nu} f(\eta), \\ \theta(\eta) &= \frac{T - T_\infty}{T_w - T_\infty}, \quad \phi(\eta) = \frac{C - C_\infty}{C_w - C_\infty}. \end{aligned} \quad (7)$$

Where $f'(\eta), \theta(\eta)$ and $\phi(\eta)$ represents the dimensionless velocity field, temperature field and concentration field. Eq. (1) is satisfied identically for $u = cx f'(\eta), v = -\sqrt{c\nu} f(\eta)$ using relation (7) into the equations (2)–(6), we achieve the differential systems as follows:

$$\left(1 - \frac{\alpha}{6} f''\right)^n f''' - \frac{n\alpha}{6} \left[1 - \frac{\alpha}{6} f''\right]^{n-1} f'' f''' - f'^2 + ff'' - Mf' = 0 \quad (8)$$

$$\left(1 + \frac{4}{3}R\right)\theta'' + \text{Pr}[f\theta' + N_b\theta'\phi' + N_t\theta'^2] + Ec \text{Pr} \left[1 - \frac{\alpha}{6} f''\right]^n f''^2 = 0, \quad (9)$$

$$\phi'' + Sc \left[f\phi' + \frac{N_t}{N_b}\theta'' - \sigma(1 + \delta\theta)^m \phi \exp\left(-\frac{E}{1 + \delta\theta}\right) \right] = 0, \quad (10)$$

$$f(0) = 0, \quad f'(0) = 1, \quad f'(\infty) \rightarrow 0, \quad (11)$$

$$\theta(0) = 1, \quad \theta(\infty) \rightarrow 0, \quad (12)$$

$$\phi(0) = 1, \quad \phi(\infty) \rightarrow 0, \quad (13)$$

here $M = \frac{\sigma^* B_0^2}{\rho_f c}$, $\text{Pr} = \frac{\nu}{\alpha}$, $R = \frac{4\sigma^* T_\infty^3}{k_f m^*}$, $N_b = \frac{\tau D_B (C_w - C_\infty)}{\nu}$, $N_t = \frac{\tau D_T (T_w - T_\infty)}{\nu T_\infty}$, $Ec = \frac{c^2 x^2}{c_p (T_w - T_\infty)}$, $Sc = \frac{\nu}{D_B}$,

$\sigma = \frac{kr^2}{c}$, $E = \frac{E_a}{\kappa T_\infty}$, $\delta = \frac{T_w - T_\infty}{T_\infty}$, magnetic parameter, Prandtl number, thermal radiation parameter,

Brownian motion parameter, thermophoresis parameter, Eckert number, Schmidt number,

dimensionless reaction rate, dimensionless activation energy and temperature difference parameter respectively.

2.1. Physical quantities

Following relations are for the resistive force (C_{fx}) as well as local Nusselt number (Nu_x):

$$C_{fx} = \frac{\tau_w}{\rho U_w^2}, \quad (14)$$

$$Nu_x = \frac{xq_w}{k(T_w - T_\infty)}, \quad (15)$$

here the τ_w, q_w shows the (wall shear stress, wall heat flux) which are expressed as:

$$\tau_w = \mu \frac{\partial u}{\partial y} \left[1 - \frac{\beta^2}{6} \left(\frac{\partial u}{\partial y} \right)^2 \right]^n, \quad (16)$$

$$q_w = -k \frac{\partial T}{\partial y} - \frac{16\sigma^{**}T_\infty^3}{3m^*} \frac{\partial T}{\partial y}. \quad (17)$$

Equating Eqs. (16) and (17) in the Eqs. (14–15), we have following non-dimensional forms of friction force and local Nusselt number:

$$C_{fx} \text{Re}_x^{1/2} = \left[1 - \frac{\alpha}{6} f''(0) \right]^n f''(0), \quad (18)$$

$$Nu_x \text{Re}_x^{-1/2} = - \left[1 + \frac{4}{3} R \right] \theta'(0). \quad (19)$$

where $\text{Re}_x = \frac{xU_w}{\nu}$ indicates local Reynolds number.

3 Entropy generation rate:

For Sutterby nanoliquid flow the entropy generation expression in dimensionless form is written as:

$$S_G = \frac{k_f}{T_\infty^2} \left[1 + \frac{16\sigma^{**}T_\infty^3}{3k_f m^*} \left(\frac{\partial T}{\partial y} \right)^2 \right] + \frac{\mu}{T_\infty} \left(\frac{\partial u}{\partial y} \right)^2 \left[1 - \frac{\beta^2}{6} \frac{\partial u}{\partial y} \right]^n + \frac{\sigma^* B_0^2 u^2}{T_\infty} + \frac{RD}{C_\infty} \left(\frac{\partial C}{\partial y} \right)^2 + \frac{RD}{T_\infty} \left(\frac{\partial T}{\partial y} \frac{\partial C}{\partial y} \right). \quad (20)$$

The above relation shows three factors (i) nanofluid resistance ir-reversibility, (ii) heat transference irreversibility and (iii) diffusive irreversibility. After using the transformation, eq. (20) can be reduced into non-dimensional form written as:

$$N_G = \alpha_1 \left[1 + \frac{4}{3} R \right] \theta'^2 + Br \left[1 - \frac{\alpha}{6} f'' \right]^n f''^2 + MBr f'^2 + \frac{\alpha_2}{\alpha_1} L \phi'^2 + L \theta' \phi', \quad (21)$$

here ($N_G = \frac{vT_\infty S_G}{\kappa C \Delta T}$, $Br = \frac{\mu U_w^2}{\kappa \Delta T}$, $\alpha_1 = \frac{\Delta C}{C_\infty}$, $\alpha_2 = \frac{\Delta T}{T_\infty}$, $L = \frac{RD(C_w - C)}{k_f}$) represents the entropy-generation rate, Brinkman number, non-dimensional concentration, temperature ratio variable and diffusive variable respectively.

The Bejan number (Be) is written as

$$Be = \frac{\alpha_1 \left[1 + \frac{4}{3} R \right] \theta'^2}{\alpha_1 \left[1 + \frac{4}{3} R \right] \theta'^2 + Br \left[1 - \frac{\alpha}{6} f'' \right]^n f''^2 + MBr f'^2 + \frac{\alpha_2}{\alpha_1} L \phi'^2 + L \theta' \phi'}. \quad (22)$$

4 Discussion

In this section, we have examined the influences of entropy generation for Sutterby fluid. Heat and mass transference features are explored by seeing features of Buongiorno's model. In order to resolve the governing equations, the numerical technique termed as bvp4c scheme is assimilated to integrate the governing ODEs.

4.1 Velocity Distribution $f'(\eta)$

Fig.1(a,b) display the features of (α) and (M) upon $f'(\eta)$. In *Fig. 1a* the behavior of Sutterby nanofluid parameter (α) against $f'(\eta)$ is exposed. Here, it is perceived that the fluid viscosity increases for larger value of α , therefore enlarged values of α produces greater resistive forces. So, decline performance is perceived in velocity profile $f'(\eta)$. *Fig.1b* is sketched to show the effects of Hartman number upon $f'(\eta)$. Same performance is detected for larger (M). Physically, Lorentz forces are associated with Hartman number, for larger values of Hartman number (M) yields more resistive forces in the transport phenomenon which declines the velocity field $f'(\eta)$.

4.2 Temperature Field $\theta(\eta)$

Fig.2(a, b) points the behavior of (N_b) and (N_t) versus $\theta(\eta)$. *Fig. 2a* shows the performance of Brownian motion parameter versus thermal field $\theta(\eta)$. A growing behavior is detected for larger value of (N_b). Physically, when Brownian motion parameter increases, particles of Sutterby nanofluid collide rapidly due to which temperature field boosted. *Fig. 2b.* designates the

impact of (N_t) upon thermal profile $\theta(\eta)$. Here, greater thermophoresis parameter (N_t) yields larger $\theta(\eta)$. From the physical point of view, in thermophoresis impression insufficient fluid particles are dragged away from hot segment toward the cold segment. Thus, huge nano-materials are move away from the concentrated area which increase the nanofluid temperature. Here, *Fig.3a* exhibits the features of (Ec) upon temperature field. Basically, Eckert number is the relationship between enthalpy difference and K.E (kinetic energy). Actually, when the value of (Ec) is augmented temperature of nanofluid is boosted. It expands change of K.E (kinetic energy) into I.E (internal energy) via work-done compared to the viscid nanofluid stresses. Enlargement in Eckert number as a result loss within heat as of plate to the nanofluid. Thus, greater energy dissipation produces larger temperature field. *Fig.3b* exhibited the significance of Prandtl number (Pr) on thermal field $\theta(\eta)$ of fluid. Because of inverse proportion among Prandtl number (Pr) plus thermal diffusivity temperature profile $\theta(\eta)$ displays decaying behavior for greater (Pr) .

4.3 Concentration profile $\phi(\eta)$

The effects of thermal radiation parameter (R) upon thermal field is exposed in *Fig.4a*. Actually, growth in thermal radiation (R) boosts $\theta(\eta)$. Physically, radiation procedure yield extra heat within the working Sutterby nanofluid thus $\theta(\eta)$ as well as associated thermal layer thickness augments. Moreover, $\phi(\eta)$ and related concentration layer diminish when Brownian motion (N_b) is intensifies (*SeeFig.4b*). *Fig.5a*. is considered to analyze the impact of chemical reaction parameter (σ) upon concentration profile $\phi(\eta)$ it is observed that concentration profile boosts for larger calculation of chemical reaction parameter (σ) . Furthermore, use of reactive species drops speedily for larger value of (σ) . Moreover, in *fig.5b* when value of diffusive variable (L) intensifies a diminishing performance is noticed for entropy generation N_G .

4.4 Entropy generation N_G and Bejan number (Be)

Attributes of (α_1) and (R) on N_G shown in *Figs.6(a,b)*. *Fig. 6a* exhibits the effects of

dimensionless temperature ratio variable (α_1) on N_G . Here, entropy generation N_G enhances for larger (α_1). Clearly, N_G increases when temperature of nanofluid enhances for larger dimensionless temperature ratio variable. Furthermore, *Fig.6b.* demonstrated the influence of (R) versus entropy generation N_G . It is evaluated that the entropy generation N_G rises when thermal radiation parameter R is intensifies. Physically, when internal energy of nanofluid is increases then the entropy generation N_G augments. *Figs.7(a,b)* depicts the impacts of (Br) versus entropy generation rate N_G as well as on Bejan number (Be). Physically, Brinkman number has ability of transferring heat in flowing liquid toward the heat transmission within molecular conduction i.e in polymer processing. Heat transport in molecular conduction is more than the heat conduction in viscid effects. So, motion of nanofluid particles yields extra heat in the close layers which augments the entropy N_G and system disorderness (*seeFig.7a*). *Fig.7b.* display that the (Be) drops for larger value of Brinkman number. The fact behind this trend is that greater Brinkman number corresponds to rise entropy rate which decays the Bejan number (Be). *Figs.8(a,b)* displays the effects of magnetic parameter on entropy generation rate N_G and Bejan number (Be). Therefore, it is perceived that N_G increases for growing value of magnetic parameter (M). Actually, increase in (M) yield further Lorentz force which rises the resistance in nanofluid flow results entropy generation rate N_G enhances (*seeFig.8a*). However, greater Hartmann number (M) displays decay in (Be). Here, nanofluid resistance is-reversibility has strong impacts upon the heat and mass transmission irreversibility thus Bejan number (Be) decays (*seeFig.8b*).

4.5 Consequence of heat and mass transference rate

Table 1: represents the impacts of few physical parameters for heat as well as mass transference. It is seen that heat transmission rate boosts for higher value of Pr , M , R and Sc whereas it decreases for higher value of Ec .

5 Final Remarks

Entropy generation rate within MHD mixed convective flow of Sutterby nanoliquid is inspected mathematically in the existence of viscous-dissipation plus thermal radiation. Following are the key points of current work:

- Sutterby nanofluid velocity profile is declining function of magnetic parameter.
- Intensifications within the values of Ec , R , Nb and Nt increases the nanofluid temperature.
- Sutterby nanofluid concentration decreased for greater Nb .
- Greater Lorentz force give augmentation to the entropy generation while declines for Bejan number.
- As compare to Bejan number, higher Br give rise to entropy generation rate.

References

- [1].Choi, S.U.S. “Enhancing thermal conductivity of fluids with nanoparticles” J. Mech. Eng., 66 (1995) pp. 99-105.
- [2].Oztop, H.F., and Abu-Nada, E. “Numerical study of natural convection in partially heated rectangular enclosures filled with nanofluids, Int. J. Heat Fluid Flow”, 29 pp. 1326-1336 (2008)
- [3].Sheikholeslami, M., Bandpy, M.G., Ellahi, R., et al. “Effects of MHD on Cu–water nanofluid flow and heat transfer by means of CVFEM” *Journal of Magnetism and Magnetic Materials* 349 pp. 188-200 (2014):
- [4].Khan, W.A., Khan, M., and Malik, R. “Three-Dimensional flow of an Oldroyd-B nanofluid towards stretching surface with heat generation/absorption” PLoS ONE, 9(8) e105107 (2014)
- [5].Makinde, O.D., Mabood, F., Khan, W.A., et al. “MHD flow of a variable viscosity nanofluid over a radially stretching convective surface with radiative heat” J. Mol. Liq. pp. 219 624-630 (2016)
- [6].Khan, M., Khan, W. A., & Alshomrani, A. S “Non-linear radiative flow of three-dimensional Burgers nanofluid with new mass flux effect” Int. J. Heat Mass Transf., 101 570-576 (2016)
- [7]. Mahanthesh, B., Gireesha B.J., and Athira, P.R. “Radiated flow of chemically reacting nanoliquid with an induced magnetic field across a permeable vertical plate” Results Phys., 7 pp. 2375-2383 (2017)
- [8].Khan, W.A., Irfan, M., Khan, M., et al. “Impact of chemical processes on magneto nanoparticle for the generalized Burgers fluid” J. Mol. Liq., pp. 234 201-208 (2017)
- [9].Mahanthesh, B., Gireesha, B.J., Shehzad, S.A., et al. “Nonlinear radiated MHD flow of

- nanoliquids due to a rotating disk with irregular heat source and heat flux condition” *Phys. B. Conden. Matt.*, pp. 537 98-104 (2018)
- [10]. Khan, W.A., Alshomrani, A.S., Alzahrani, A.K., et al. “Impact of autocatalysis chemical reaction on nonlinear radiative heat transfer of unsteady three-dimensional Eyring-Powell magneto-nanofluid flow” *Pramana-J. Phys.*, 91 pp. 63 (2018) doi.org/10.1007/s12043-018-1634-x.
- [11]. Khan, W.A., Sultan, F., Ali, M., et al., “Consequences of activation energy and binary chemical reaction for 3D flow of Cross-nanofluid with radiative heat transfer” *J. Braz. Soc. Mech. Sci. Eng.*, 41 (2019) 4: doi.org/10.1007/s40430-018-1482-0.
- [12]. Khan, W.A., Waqas, M., Ali, M., et al. “Mathematical analysis of thermally radiative time-dependent Sisko nanofluid flow for curved surface” *Int. J. Numer. Methods Heat Fluid Flow*, 29(9) pp. 3498-3514 (2019)
- [13]. Chu, Y. M., Bilal, S., & Hajizadeh, M. R. “Hybrid ferrofluid along with MWCNT for augmentation of thermal behavior of fluid during natural convection in a cavity” *Math. Methods Appl. Sci.*, (2020) <https://doi.org/10.1002/mma.6937>.
- [14]. Khan, W.A., Ali, M., Shahzad, M., et al. “A note on activation energy and magnetic dipole aspects for Cross nanofluid subjected to cylindrical surface, *Appl Nanosci* 10 pp. 3235-3244 (2020)
- [15]. Khan, M. I., Shah, F., Khan, S. U., et al. “Heat and mass transfer analysis for bioconvective flow of Eyring Powell nanofluid over a Riga surface with nonlinear thermal features” *Numer. Methods Partial Differ. Equ.*, (20220): doi.org/10.1002/num.22696.
- [16]. Khan, W. A., Farooq, S., Kadry, S., et al. “Variable characteristics of viscosity and thermal conductivity in peristalsis of magneto-Carreau nanoliquid with heat transfer irreversibilities” *Comput. Meth. Prog. Bio.*, pp. 190 105355 (2020)
- [17]. Khan, W.A., Sun, H ., Shahzad, M., et al. “Importance of heat generation in chemically reactive flow subjected to convectively heated surface” *Indian J Phys*, 95, pp. 89–97 (2021) <https://doi.org/10.1007/s12648-019-01678-2>
- [18]. Peng, Y., Ghahnaviyeh, M.B., Ahmad, M.N., et al. “Analysis of the effect of roughness and concentration of Fe₃O₄/water nanofluid on the boiling heat transfer using the artificial neural network: An experimental and numerical study” *Int. J. Therm. Sci.*, 163 pp. 106863 (2021)
- [19]. Chu, Yu-Ming., Nazir, U., Sohail, M., et al. “Enhancement in thermal energy and solute

- particles using hybrid nanoparticles by engaging activation energy and chemical reaction over a parabolic surface via finite element approach” *Fractal Fract.*, 5 (3) (2021) 119: doi.org/10.3390/fractalfract5030119.
- [20]. Khan, W.A., Anjum, N., Waqas, M., et al. “Impact of stratification phenomena on a nonlinear radiative flow of sutterby nanofluid” *J. Mater. Res. Technol.*, 15 pp. 306-314 (2021)
- [21]. Anjum, N., Khan, W. A., Ali, M., et al. “Thermal performance analysis of Sutterby nanoliquid subject to melting heat transportation” *International Journal of Modern Physics B*, pp.2350185 (2022)
- [22]. Hussain, Z., Ali, M., and Khan, W.A., “Significance of Chemical Processes and Non-uniform Heat Sink/source Aspects for Time-dependent Polymer Liquid Carrying Nanoparticles” *Journal of Magnetism*, 27, no. 4, pp. 347-355 (2022)
- [23]. Chu, Yu-Ming., Bashir, S., Ramzan, M., et al. “Model-based comparative study of magnetohydrodynamics unsteady hybrid nanofluid flow between two infinite parallel plates with particle shape effects” *Math. Methods Appl. Sci.*, (2022): doi.org/10.1002/mma.8234.
- [24]. Nazeer, M., Hussain, F., Khan, M.I., et al. “Theoretical study of MHD electro-osmotically flow of third-grade fluid in micro channel” *Appl. Math. Comput.* , 420 pp.126868 (2022)
- [25]. Chu, Yu-Ming., Shankaralingappa, B.M., Gireesha, B.J., et al. “Combined impact of Cattaneo-Christov double diffusion and radiative heat flux on bio-convective flow of Maxwell liquid configured by a stretched nano-material surface” *Appl. Math. Comput.* 419 pp.126883 (2022)
- [26]. Khan, W.A., Ahmad, A., Anjum, N., et al. “Impact of nanoparticles and radiation phenomenon on viscoelastic fluid” *Int. J. Mod. Phys. B*, 36 (05) pp.2250049 (2022)
- [27]. Hussain, Z., Khan, W.A., Muhammad, T., et al. “Dynamics of gyrotactic microorganisms for chemically reactive magnetized 3D Sutterby nanofluid fluid flow comprising non-uniform heat sink-source aspects” *Journal of Magnetism and Magnetic Materials*, pp.170798 (2023)
- [28]. Hussain, Z., Alam, M., Pasha, A.A., et al. “Gyrotactic microorganisms analysis for radiative 3D Carreau nanofluid flow configured by activation energy and viscous dissipation” *Thermal Science and Engineering Progress*, pp.101898 (2023)
- [29]. Hussain, Z., Khan, W. A., and Ali. M., Thermal radiation and heat sink/source aspects on 3D magnetized Sutterby fluid capturing thermophoresis particle deposition. *International Journal of Modern Physics B*, pp. 2350282 (2023)

- [30]. Anjum, N., Khan, W. A., Azam, M., et al. "Significance of bioconvection analysis for thermally stratified 3D Cross nanofluid flow with gyrotactic microorganisms and activation energy aspects" *Thermal Science and Engineering Progress*, 38 pp.101596 (2023)
- [31]. Pasha, A.A., Hussain, Z., Alam, Md.M., et al. "Impact of magnetized non-linear radiative flow on 3D chemically reactive sutterby nanofluid capturing heat sink/source aspects" *Case Studies in Thermal Engineering*, 41 pp.102610 (2023)
- [32]. Khan, W. A., and Ali, M. "Recent developments in modeling and simulation of entropy generation for dissipative cross material with quartic autocatalysis" *Applied Physics A*, 125 pp.1-9 (2019):
- [33]. Khan, M.I., Qayyum, S., Chu, Yu-Ming, et al. Numerical simulation and modeling of entropy generation in Marangoni convective flow of nanofluid with activation energy, *Numer. Methods Partial Differ. Equ.*, (2020) <https://doi.org/10.1002/num.22610>.
- [34]. Khan, W.A., Khan, M.I., Kadry, S., et al. "Transportation of water-based trapped bolus of SWCNTs and MWCNTs with entropy optimization in a non-uniform channel" *Neural. Comput. Applic.*, 32 pp.13565-13576 (2020)
- [35]. Shahzad, M., Sun, H., Sultan, F., et al. "Transport of radiative heat transfer in dissipative Cross nanofluid flow with entropy generation and activation energy", *Phys. Scr.*, 94 pp.115224 (2019)
- [36]. Zhao, T.H., Khan, M.I., and Chu, Y.M. "Artificial neural networking (ANN) analysis for heat and entropy generation in flow of non-Newtonian fluid between two rotating disks" *Math. Methods Appl. Sci.*, (2021) <https://doi.org/10.1002/mma.7310>.
- [37]. Qayyum, S., Khan, M.I., Masood, F., et al. "Interpretation of entropy generation in Williamson fluid flow with nonlinear thermal radiation and first-order velocity slip" *Math. Methods Appl. Sci.*, 44 (9) pp. 7756-7765 (2021)
- [38]. Wang, J., Khan, W.A., Asghar, Z., et al. "Entropy optimized stretching flow based on non-Newtonian radiative nanoliquid under binary chemical reaction" *Comput. Meth. Prog. Bio.*, 188 pp.105274 (2020)
- [39]. Khan, W.A., Waqas, M., Kadry, S., et al. "On the evaluation of stratification-based entropy optimized hydromagnetic flow featuring dissipation aspect and Robin conditions" *Comput. Meth. Prog. Bio.*, 190, pp. 105347 (2020)
- [40]. Qayyum S., Khan M.I., Masood F., et al. "Interpretation of entropy generation in

Williamson fluid flow with nonlinear thermal radiation and first-order velocity slip” *Math. Methods Appl. Sci.*, (2020): doi.org/10.1002/mma.6735.

- [41]. Shah, F., Khan M.I., Chu Y.M. et al. “Heat transfer analysis on MHD flow over a stretchable Riga wall considering Entropy generation rate: a numerical study” *Numer. Methods Partial Differ. Equ.*, (2020) <https://doi.org/10.1002/num.22694>.
- [42]. Hussain, Z., Khan W. A., Ali M., et al. "Simultaneous features of nonuniform heat sink/source and activation energy in entropy optimized flow of Sutterby fluid subject to thermal radiation." *International Journal of Modern Physics B*, pp. 2350208 (2023)
- [43]. Waqas, M., Sunthrayuth P., Pasha A.A., et al. “Entropy generation analysis for the radiative flow of Sisko nanofluid with heat sink/source” 2022: doi.org/10.1080/17455030.2022.2094026.

Biographies

Waqar Azeem Khan is an Assistant professor at Mohi Ud Din Islamic University (MIU), Nerian Sharif, A.J.K, Pakistan. He received PhD in Mathematics, Quaid-i-Azam University, Islamabad, Pakistan. His research interests included is Fluid Mechanics. His published 200 research articles appear in reputable international journals.

Nazash Anjum Ph.D student in the Department of Mathematics, Mohi Ud Din Islamic University (MIU), Nerian Sharif. A.J.K, Pakistan. His current research interests in Fluid Mechanics.

Aatef Hobiny is an Assistant professor at King Abdulaziz University, Saudi Arab. His research interests included is Fluid Mechanics and. His published research articles appear in reputable international journals.

Mehboob Ali is an Assistant professor at Guangxi Minzu University, Nanning, China. He received PhD in Mathematics, Hazara University, Mansehra, Pakistan. His research interests included is Physical Chemistry, Fluid Mechanics and Mathematical Modeling. His published 85 research articles appear in reputable international journals.

Nomenclature			
u, v	Velocity components	η	dimensionless variable
x, y	Space coordinates	U_w	stretching velocity
ρ	Density of fluid	Pr	Prandtl number
ν	Kinematic viscosity	M	Magnetic parameter
μ	Dynamic viscosity	Nr	Buoyancy Ratio Parameter
Γ	Material constant	$GDQM$	Generalized differential quadrature method
B_0	Uniform magnetic field strength	R	thermal radiation parameter
$(\rho c)_f$	Heat capacity of fluid	N_b	Brownian motion parameter
τ	Ratio of heat capacity	N_t	thermophoresis parameter
$(\rho c)_p$	Effective heat capacity	Ec	Eckert Number
α_1	thermal diffusivity	Sc	Schmidth Number
σ^{**}	Stefan-Boltzmann constant	σ	Reaction rate
α	thermal diffusivity	E	Activation energy
k_f	thermal conductivity	δ	Temperature Difference Parameter
c_p	specific heat capacity	τ_w	Wall shear-stress
D_B, D_T	Brownian, thermophoresis	q_w	Wall heat-flux
T, C	temperature, concentration	f	dimensionless Velocitie
T_∞	ambient temperature	θ	Dimensionless temperature

C_∞	ambient concentration	ϕ	Dimensionless concentration
T_w	surface temperature	N_G	Entropy generation rate
C_w	surface concentration	α_2	temperature ratio parameter
$k_{r,2}$	reaction rate	α_1	concentration ratio parameter
E_a	activation energy	L	Diffusive variable
Γ	Time material constant	Br	Brinkman number
κ	Boltzmann constant	C_{fx}	skin friction
k_c	rate of chemical reaction	Nu_x	local Nusselt number
m	fitted rate constant	Re_x	local Reynolds number
c	dimensional constant		

List of Table

Table 1: Values of Local Nusselt number and Sherwood number for different values of the parameters Pr, M, Nb, Sc and Ec when $M = \lambda = Nt = \alpha = 0.1$.

List of Figures

Fig.1(a,b). Impact of α and M on $f'(\eta)$.

Fig.2(a,b). Effects of N_b and N_t upon $\theta(\eta)$.

Fig.3(a,b). Influence of Ec and Pr against $\theta(\eta)$.

Fig.4(a,b). Effects of R and N_B upon $\theta(\eta)$ and $\phi(\eta)$.

Fig.5(a,b). Impact of σ and L upon $\phi(\eta)$ and N_G .

Fig.6(a,b). Impacts of α_1 and R upon N_G .

Fig.7(a,b). Effects of Br versus N_G and (Be) .

Fig.8(a,b). Consequence of M versus N_G and (Be) .

List of Table

Table 1: Values of Local Nusselt number and Sherwood number for different values of the parameters Pr, M, Nb, Sc and Ec when $M = \lambda = Nt = \alpha = 0.1$.

Pr	M	N_b	Sc	Ec	$-\theta'(0)$	$-\phi'(0)$
0.5	0.1	0.1	0.1	0.1	-0.27252	-0.340371
0.6					-0.30199	-0.339589
0.7					-0.35901	-0.325297
0.5	0.2				-0.28458	-0.330763
	0.3				-0.27805	-0.330543
	0.4				-0.272	-0.33035
		0.2			-0.28518	-0.337229
		0.3			-0.2788	-0.339316
		0.4			-0.27252	-0.340371
			0.2		-0.29141	-0.351474
			0.3		-0.29118	-0.372936
			0.4		-0.29096	-0.395071
				0.2	-0.27107	-0.332987
				0.3	-0.25047	-0.334961
				0.4	-0.22987	-0.336936

List of Figures

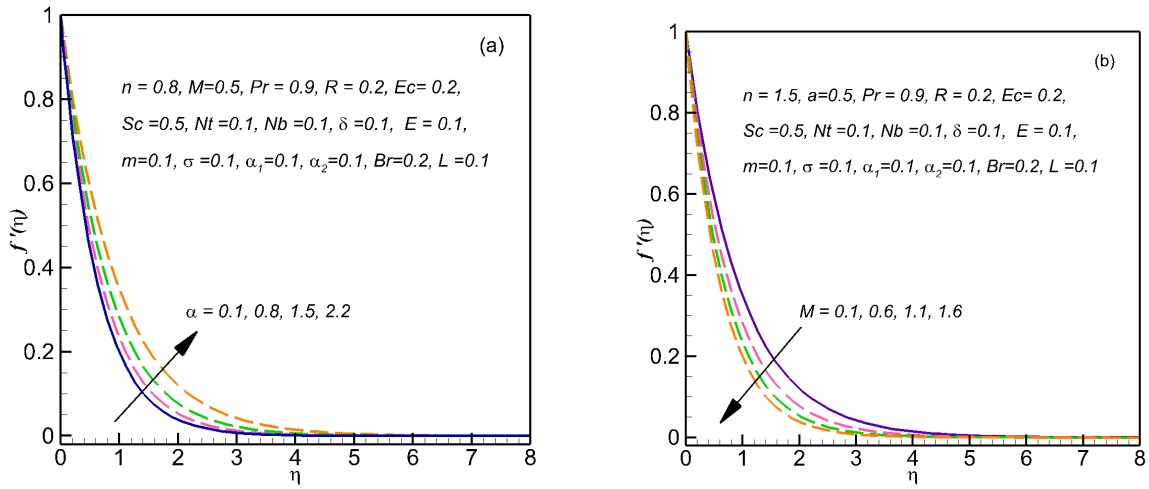


Fig.1(a,b). Impact of α and M on $f'(\eta)$.

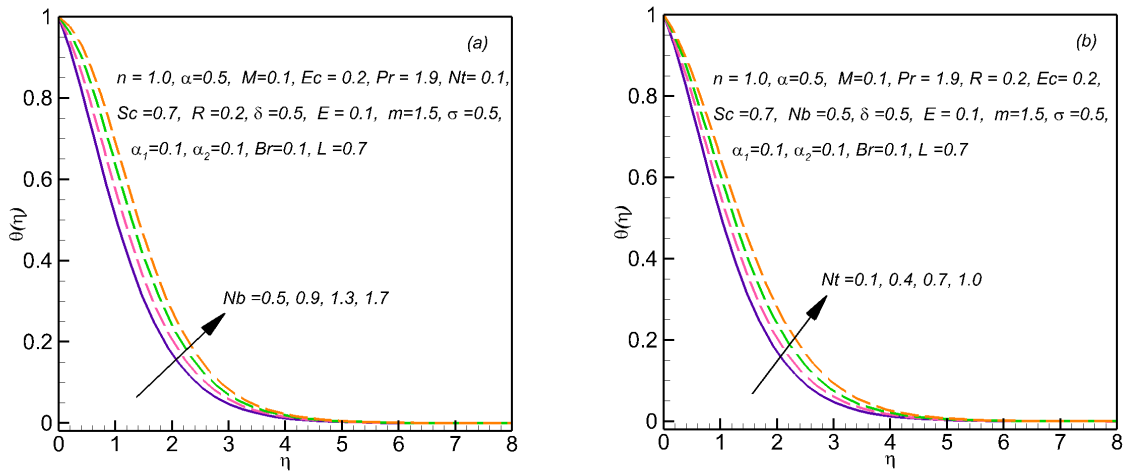


Fig.2(a,b). Effects of N_b and N_t upon $\theta(\eta)$.

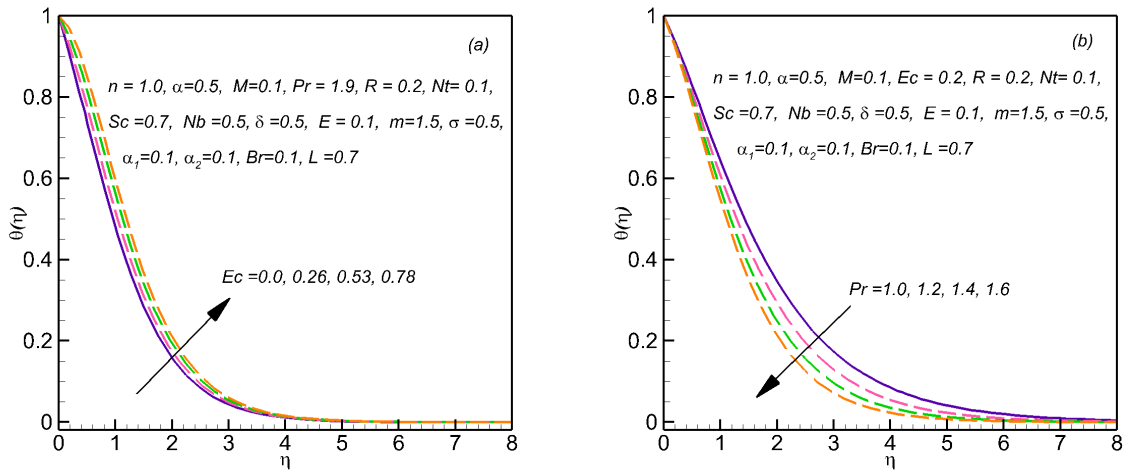


Fig.3(a,b). Influence of Ec and Pr against $\theta(\eta)$.

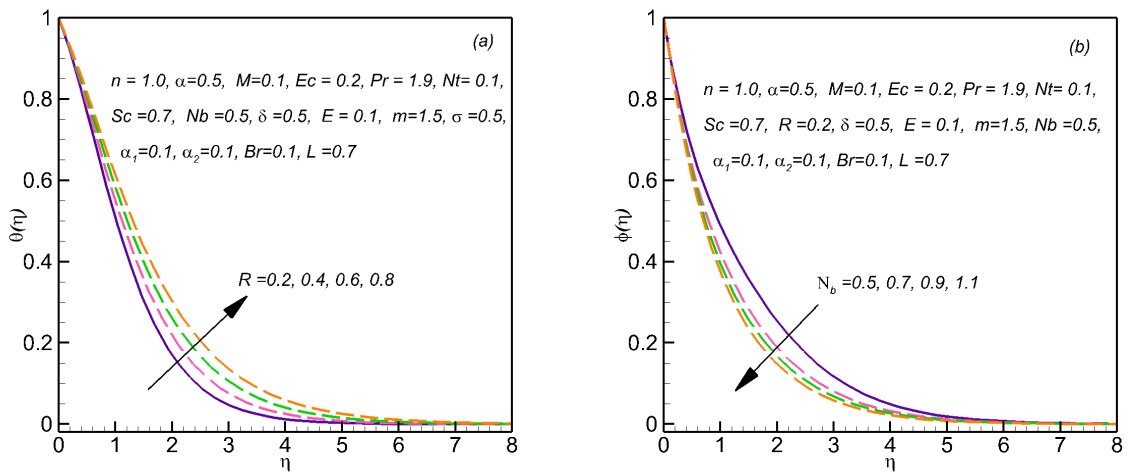


Fig.4(a,b). Effects of R and N_B upon $\theta(\eta)$ and $\phi(\eta)$.

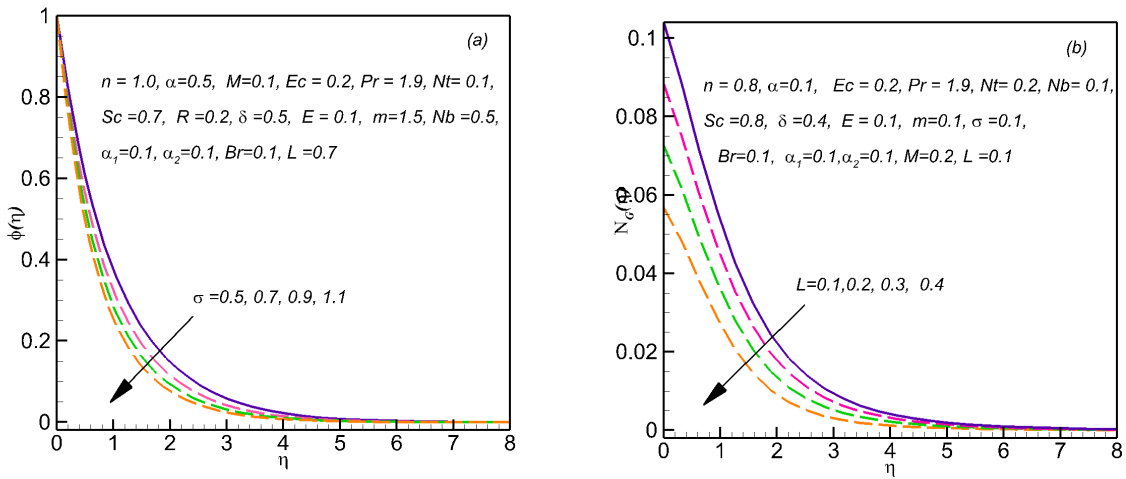


Fig.5(a,b) . Impact of σ and L upon $\phi(\eta)$ and N_G .

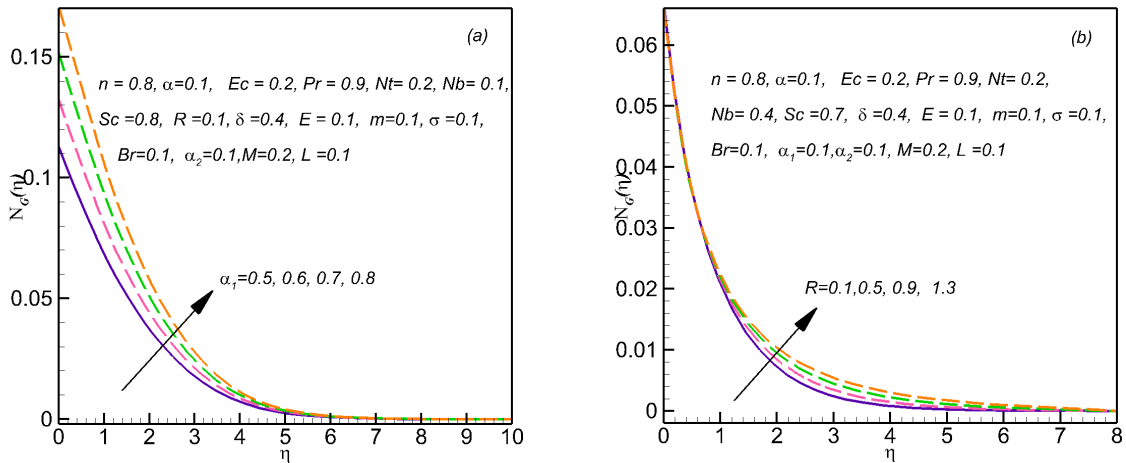


Fig.6(a,b) . Impacts of α_1 and R upon N_G .

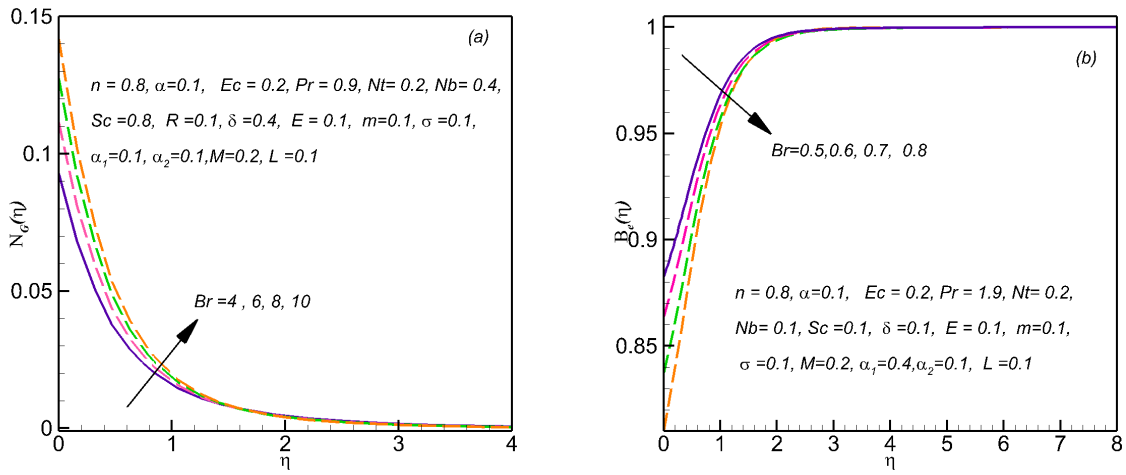


Fig.7(a,b) . Effects of Br versus N_G and (Be) .

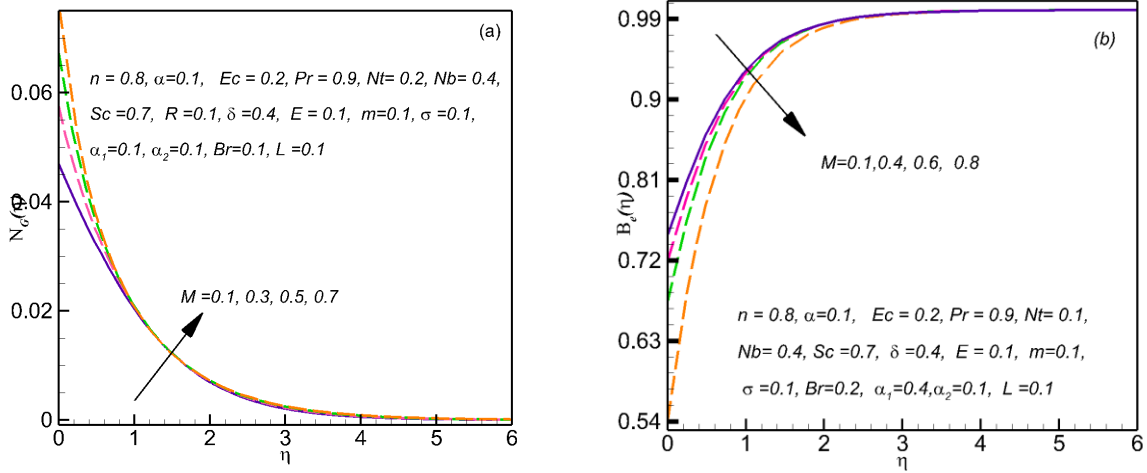


Fig.8(a,b) . Consequence of M versus N_G and (Be) .